

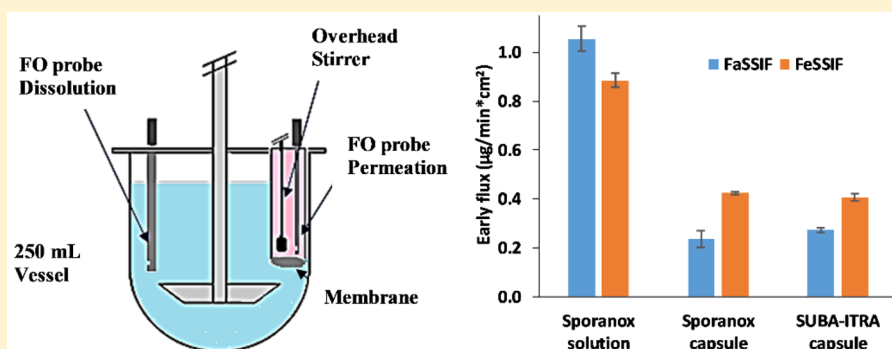
# Prediction of Bioequivalence and Food Effect Using Flux- and Solubility-Based Methods

Enikő Borbás,<sup>\*,†,‡</sup> Szabina Kádár,<sup>†</sup> Konstantin Tsinman,<sup>‡</sup> Oksana Tsinman,<sup>‡</sup> Dóra Csicsák,<sup>§</sup> Krisztina Takács-Novák,<sup>§</sup> Gergely Völgyi,<sup>§</sup> Bálint Sinkó,<sup>\*,‡</sup> and Hajnalka Pataki<sup>†,‡</sup>

<sup>†</sup>Department of Organic Chemistry and Technology, Budapest University of Technology and Economics, Budapest H-1111, Hungary

<sup>‡</sup>Pion Inc, Billerica, Massachusetts 01821, United States

<sup>§</sup>Department of Pharmaceutical Chemistry, Semmelweis University, Budapest H-1092, Hungary



**ABSTRACT:** In this work, two different approaches have been developed to predict the food effect and the bioequivalence of marketed itraconazole (ITRA) formulations. Kinetic solubility and simultaneous dissolution–permeation tests of three (ITRA) formulations (Sporanox capsules and solution and SUBA-ITRA capsules) were carried out in simulated fasted and fed states. Fraction of dose absorbed ratios estimating food effect and bioequivalence were calculated based on these results and were compared to the *in vivo* study results published by Medicines Agencies. The comparison demonstrated that kinetic solubility and flux values could be used as input parameters for biopharmaceutics modeling and simulations to estimate food effect and bioequivalence. Both prediction methods were able to determine a slightly negative food effect in the case of the Sporanox solution and also a pronounced positive food effect for the Sporanox capsule. Superior bioavailability was predicted when the Sporanox solution was compared to the Sporanox capsule (in agreement with *in vivo* data).

**KEYWORDS:** BioFLUX, dissolution–permeation, membrane transport, absorption, itraconazole, supersaturation, kinetic solubility, *in vivo*, *in vitro*, prediction, fraction of dose absorbed

## 1. INTRODUCTION

Improving the *in vivo* predictive power of dissolution tests for biopharmaceutics classification system (BCS) class II type drugs has become one of the major challenges of the pharmaceutical industry.<sup>1,2</sup> Among the underlying reasons for the poor *in vivo* predictive power is the use of solubilizing agents, such as surfactants, bile salts, cyclodextrins (CD) or even polymers, that may influence not only the dissolution and the solubility but also the membrane transport of such solubility limited active pharmaceutical ingredients (API).<sup>3–8</sup> Solubility limited cases can further be categorized based on the limiting step of transport: unstirred water layer (UWL) or epithelial membrane permeation.<sup>3,9,10</sup> In cases of lipophilic compounds where cellular membrane permeation is very fast, UWL permeation is often the rate-limiting step of absorption.<sup>11–15</sup> While the bile micelles and CDs usually increase the solubility of lipophilic compounds it has been realized that they decrease the effective permeability ( $P_{\text{eff}}$ ) due

to a reduction of the fraction of free drug at the epithelial membrane surface and/or the reduction of the diffusion coefficient in the UWL caused by the enlarged hydrodynamic radius of the micelle or CD complex as compared to the pure API.<sup>16–26</sup> Therefore, the balance of the solubility increase and the  $P_{\text{eff}}$  decrease determines the direction and the extent of the food or CD effect.<sup>17</sup>

Part of the gastrointestinal unified theoretical (GUT) framework mathematical model, assuming that both free drug and micelle bound drug permeate through the UWL by self-diffusion was found to be appropriate for the prediction of the fraction of dose absorbed ( $F_a$ ) in the cases of lipophilic drugs with UWL limited absorption, by Sugano et al.<sup>10,27</sup>

**Received:** April 16, 2019

**Revised:** September 13, 2019

**Accepted:** September 16, 2019

**Published:** September 16, 2019

There have been many attempts to characterize formulations with novel *in vitro* tests and apparatuses better. For poorly water-soluble compounds, the determination of kinetic solubility, i.e., the maximum concentration in a supersaturated solution that can be obtained at the moment of precipitation,<sup>28</sup> is of high importance. When an excess amount of API is added to such a solution and a new amorphous phase is forming, this solubility value is called amorphous instead of kinetic.<sup>29</sup> The supersaturation ratio<sup>4,30</sup> (the ratio of the dissolved amount of the drug relative to its equilibrium crystalline solubility measured in the same media) may be valuable information in terms of characterizing the API. Solubility tests have also been applied to assess the effect of formulation excipients on the extent and duration of supersaturation.<sup>31,32</sup> Although it has been suggested that kinetic or amorphous solubility data may be useful to estimate bioavailability enhancement caused by the amorphization of the API,<sup>29,33,34</sup> this data has only been used sparsely as an input parameter for prediction of  $F_a$  and food effect,<sup>35</sup> and has never been used to estimate the bioequivalence of generic drug products.

In recent years, many new *in vitro* tools have been developed to improve the *in vitro* *in vivo* correlation (IVIVC) by the simultaneous testing of dissolution and absorption.<sup>36,37</sup> The parallel artificial membrane permeability assay (PAMPA) has been shown to be predictive of passive transcellular permeability,<sup>38</sup> while having the advantage of being a reproducible and cost-effective way of testing formulations compared to cell-based assays or animal tests. Therefore, it was proposed that a scaled-up version of a PAMPA-like setup could become a way of combining dissolution and absorption testing. A small volume (16–20 mL) side-by-side diffusion cell apparatus called  $\mu$ FLUX, and a large volume (850–1000 mL) version MacroFLUX, was recently developed and proven to be a valuable tool in formulation development.<sup>4,30,39–42</sup> The BioFLUX apparatus was a novel device that incorporates an absorption compartment into a USP II dissolution apparatus, like MacroFLUX, while changing the working volume in the dissolution vessel from 900 mL to a more biorelevant 250 mL.<sup>9,43,44</sup> Flux data generated with this setup has not yet been published. Although by enabling simultaneous measurement of dissolution and absorption rates, it has the potential to improve IVIVC.<sup>41,39</sup> Flux values have yet been sparsely used as an input parameter in a predictive model for the calculation of food effect and bioequivalence from an oral dosage form.

Itraconazole (ITRA), a BCS II class antifungal drug, was chosen as a model compound. ITRA is a very lipophilic weak base ( $pK_a = 3.87$ )<sup>41</sup> with extremely low aqueous solubility and pH-dependent permeability.<sup>45</sup> The first commercial solid formulation of ITRA, Sporanox capsules, (Janssen Pharmaceutica, Beerse, Belgium) contain the API in amorphous form dispersed with hydroxypropylmethylcellulose (HPMC) on sugar spheres.<sup>46</sup> This formulation uses the advantage of the high surface area of small spray-dried particles dispersed on the sugar spheres, and also the amorphous state to improve drug dissolution. The capsule formulation is supposed to be taken after a full meal,<sup>47</sup> which limits its utility as patients being unable to take solid food are excluded. In contrast, Sporanox oral solution, marketed 5 years after the capsule, has shown higher bioavailability in the fasted state than in the fed state, and therefore may be advantageous in therapy for such patients.<sup>48</sup>

The oral solution contains 10 mg/mL ITRA in a pH 2 media. In order to reach around a four magnitude higher

concentration in solution than the thermodynamic solubility of the crystalline drug at that pH, the formulation contains 400 mg/mL of (2-hydroxypropyl)- $\beta$ -cyclodextrin (HP- $\beta$ -CD).<sup>47,48</sup> The oral bioavailability of ITRA when administered as oral solution and capsule dosage forms was 35% and 10% in rats, respectively.<sup>49,50</sup> The absolute oral bioavailability of Sporanox solution in the fed state when administered to humans was found to be 55%.<sup>47,48</sup> Human data also showed a significant difference between the bioavailability of the solution and capsule forms; therefore, the solution and capsule dosage forms are not bioequivalent and cannot be used interchangeably.<sup>47,48</sup>

SUBA-Itraconazole (SUBA-ITRA) is a novel amorphous solid dispersion (ASD) containing ITRA in a pH-dependent polymeric matrix (hydroxypropylmethylcellulose-phthalate, HPMC-P) to enhance its dissolution and intestinal absorption. Although with a halved dose compared to the innovator product (Sporanox capsules), it has failed to meet bioequivalence criteria but showed therapeutic equivalence.<sup>51</sup> Currently, it is available in Australia and Germany under the trade name Lozanoc (Mayne Pharma Ltd.), and in Spain as Itragerm.

The aim of this study was to predict food effect and bioequivalence for three marketed formulations of ITRA (Sporanox capsules, Sporanox solution, SUBA-ITRA capsules) by using the results of state of the art experimental techniques, like kinetic solubility and simultaneous dissolution–absorption measurements, as input parameters for biopharmaceutics modeling and simulations, and then to compare the performance of the different approaches.

## 2. EXPERIMENTAL SECTION

**2.1. Materials.** Crystalline itraconazole (ITRA) (706 g/mol, structure shown in Figure 1) and buffer components

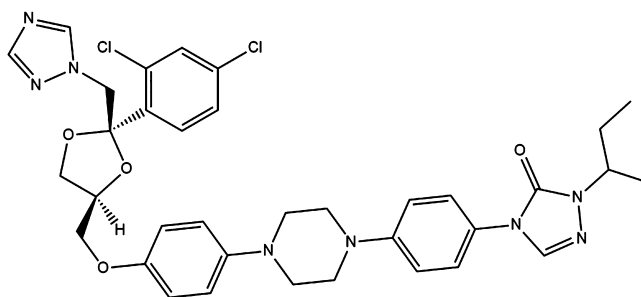


Figure 1. Structure of itraconazole.

( $\text{NaH}_2\text{PO}_4$ , NaOH, NaCl, KCl, HCl) were purchased from Sigma-Aldrich Co. LLC. (St. Louis, MO, USA). (2-Hydroxypropyl)- $\beta$ -cyclodextrin (HP- $\beta$ -CD), with the molar substitution degree = 0.64, was purchased from Roquette Frères (Lestrem, France). Hydroxypropyl methylcellulose (HPMC 2910) was obtained from Aqualon, Hercules (Zwijndrecht, The Netherlands), and hydroxypropyl methylcellulose-phthalate (HPMC-P) was purchased from Shin-Etsu Pharma & Food Materials Distribution GmbH (Wiesbaden, Germany). The gastrointestinal tract (GIT) lipid and acceptor sink buffer (ASB) were obtained from Pion Inc. (Billerica, MA, USA). Simulated intestinal fluid (SIF) powder was purchased from Biorelevant.com (London, U.K.). Itraconazole marketed formulations were purchased from the listed companies: Sporanox solution and capsules from Johnson & Johnson (Beerse, Belgium), SUBA-Itraconazole capsules from Mayne

Pharma (Salisbury, Australia). Table 1 summarizes the composition of the ITRA containing marketed formulations.

**Table 1. Composition of Itraconazole Containing Marketed Formulations**

formulation	dose (mg/capsule)	main additive	load of additive
Sporanox solution	100 mg/10 mL	HP- $\beta$ -CD	4000 mg/10 mL <sup>47,48</sup>
Sporanox capsules	100	HPMC 2910	not published
SUBA-ITRA capsules	50	HPMC-P	75 mg/capsule <sup>52</sup>

**2.2. Methods.** **2.2.1. Solubility Assays.** **2.2.1.1. Thermodynamic Solubility Assay.** The saturation shake flask (SSF) method<sup>53,54</sup> was used to determine the thermodynamic solubility of ITRA in pH 1.2 simulated gastric fluid (SGF), in pH 6.5 phosphate buffer (FaSSIF blank), pH 5 acetate buffer (FeSSIF blank) and pH 7.4 ASB. The sample was added in excess to the aqueous buffer solutions to produce a suspension. At a controlled temperature of  $37.0 \pm 0.1$  °C, the solution containing solid excess of the sample was vigorously stirred for a period of 6 h, followed by a further sedimentation period of 18 h (stirrer turned off). Three aliquots were carefully withdrawn from the liquid using a fine glass pipet and were diluted with solvent as necessary. The concentration of the saturated solution was measured by UV spectroscopy using a JASCO V 550 UV/vis spectrophotometer. Three replicate solubility measurements were carried out at each of the tested conditions. The solid phase after the assay was not characterized.

**2.2.1.2. Kinetic Solubility Measurements.** Note that, in the context of this work, solubility measured by this method will be called kinetic solubility because the form of the solid phase precipitating during these assays was not characterized. A concentrated (1 mg/mL) stock solution of ITRA was prepared using 2 N HCl solution as a solvent. Ten mL of dissolution medium was stirred at 200 rpm and held at 37 °C by circulating water through a heating block mounted to a Pion  $\mu$ DISS profiler (Pion Inc., Billerica, MA). The stock solution was added in 5  $\mu$ L aliquots to the equilibrated FaSSIF or FeSSIF buffer containing predissolved additives (15.4 mg/mL HP- $\beta$ -CD or 300  $\mu$ g/mL HPMC 2910 or 300  $\mu$ g/mL HPMC-P). To readjust the pH of the media after every addition of the stock solution, 1 N NaOH was used. During and after addition of the stock solution, UV probes connected to a Pion Rainbow Dynamic Dissolution Monitor (Pion Inc., Billerica, MA) system were used to detect changes in UV spectra thus

enabling the detection of precipitation, which provides information about the kinetic solubility limit. Light scattering was detected by monitoring the extinction at nonabsorbing wavelengths (400 nm).

**2.2.2. Flux Experiments.** Marketed formulations of ITRA were tested using BioFLUX (Pion Inc., Billerica, MA). In this device, the acceptor compartment is integrated with a permeable membrane, an overhead stirrer, and a fiber optic UV probe (10 mm path length), which is then inserted into the 500 mL vessel of a USP II apparatus (Erweka DT 126 Dissolution Tester, Heusenstamm Germany) (Figure 2). A scaled-up version of the PAMPA membrane, which previously has shown good compatibility with formulation excipients like HP- $\beta$ -CD and biorelevant media, was chosen as the integrated membrane.<sup>39,55</sup> This artificial GIT-mimicking membrane was formed by impregnating the filter support (hydrophobic PVDF, polyvinylidenefluoride, 0.45  $\mu$ m pore size, 3.69 cm<sup>2</sup>) with 50  $\mu$ L of GIT lipid solution (Pion Inc., Billerica, MA). This membrane was separating the dissolution (donor) compartment from the acceptor compartment containing 20 mL of pH 7.4 ASB (Pion Inc., Billerica, MA). In the case of the fasted state, the experiment began in 200 mL of pH 1.6 buffer, simulating gastric conditions (SGF) on the donor side. For the initial 30 min of the experiment, the acceptor compartment was not connected to the donor compartment. After 30 min the media in the dissolution vessel was converted to fasted state simulated intestinal fluid (FaSSIF V1) (pH 6.5) by adding 50 mL of a specially formulated concentrate<sup>42</sup> containing SIF powder (biorelevant.com); the acceptor compartment was then added to begin the permeation experiment. In the case of fed state assays, 250 mL of fed state simulated intestinal fluid (FeSSIF V1) was used in the donor compartment. No media change was carried out, and the acceptor compartment was assembled into the dissolution vessel from the beginning of the experiments. On the basis of the USP recommendation for ITRA containing capsules, a stirring speed of 100 rpm was selected for agitation of the donor compartment.<sup>56</sup> To study the efficiency of stirring in the acceptor compartment, the flux data for a highly permeable model compound, propranolol, was compared for 0, 250, 450, and 600 rpm stirring speeds. There was a significant difference between the flux results in the case of stirring and nonstirring, though the results were found to be within the standard deviation of each other for every stirring speed (250, 450, and 600 rpm). Thus, the rate of 450 rpm was selected for all assays. The integrated fiber-optic (FO) UV probes were positioned in the donor and acceptor compartments and connected to the Rainbow Dynamic Dissolution Monitor instrument (Pion Inc.,

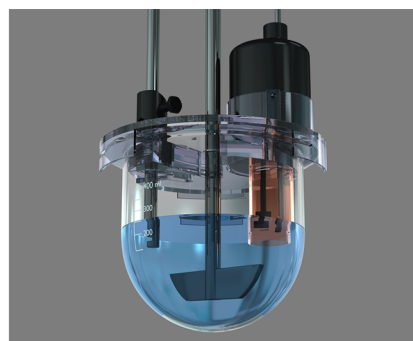
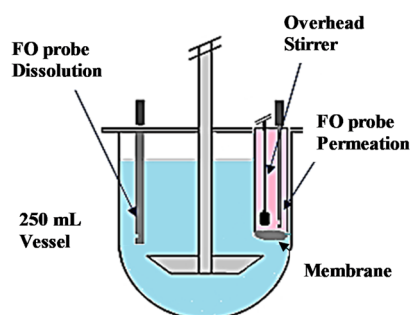


**Figure 2.** Schematic (on the left) and image (on the right) of the dissolution–flux device used in this study (BioFLUX).



Billerica, MA, USA), enabling real-time concentration monitoring. The flux ( $J$ ) across the membrane was calculated using the following equation:

$$J(t) = \frac{dm}{Adt} \quad (1)$$

where the flux of a drug through the membrane is defined as the amount ( $m$ ) of drug crossing a unit area ( $A$ ) perpendicular to its flow per unit time ( $t$ ). Early fluxes were calculated from the linear portion of the appearance profiles (50–120 min).

**2.2.3. Estimation of Fraction Absorbed Ratios Based on Sugano's Method.**<sup>9,10</sup> The fraction absorbed ( $F_a$ ) ratio for the prediction of food effect from the same formulation can be estimated:<sup>9</sup>

$$F_a \text{ ratio} \approx \frac{P_{UWL, \text{fed}}}{P_{UWL, \text{fasted}}} \times \frac{S_{\text{fed}}}{S_{\text{fasted}}} \times \frac{V_{GI, \text{fed}}}{V_{GI, \text{fasted}}} \quad (2)$$

where  $P_{UWL}$  is the unstirred water layer permeability of the drug,  $S$  is the solubility, and  $V_{GI}$  is the effective fluid volume in the gastrointestinal tract in fed or fasted conditions denoted by corresponding subscripts.

The food effect prediction approach published by Sugano et al.<sup>9</sup> Equation 2 was adapted in this study to calculate  $F_a$  ratio for predicting bioequivalence (eq 3):

$$F_a \text{ ratio} \approx \frac{P_{UWL, \text{test}}}{P_{UWL, \text{reference}}} \times \frac{S_{\text{test}}}{S_{\text{reference}}} \quad (3)$$

where parameters of the test and reference drug product can be substituted accordingly.

Effective UWL permeability in a particular medium would be proportional to the effective diffusivity of the API containing complexes ( $D_{UWL, \text{eff}}$ ), and reversely proportional to the effective thickness of UWL,  $h_{\text{eff}}$ :

$$P_{UWL, \text{eff}} = \frac{D_{UWL, \text{eff}}}{h_{\text{eff}}} = \frac{(f_{\text{mono}} \times D_{UWL, \text{mono}} + f_{\text{mic}} \times D_{UWL, \text{mic}})}{h_{\text{eff}}} \quad (4)$$

where  $f_{\text{mono}}$  and  $f_{\text{mic}}$  are the fractions of the free monomer and micelle bound API correspondingly ( $f_{\text{mono}} + f_{\text{mic}} = 1$ ), while  $D_{UWL, \text{mono}}$  and  $D_{UWL, \text{mic}}$  are the diffusion coefficients of the free monomer and micelle bound drug in the UWL.

The  $f_{\text{mono}}$  can be estimated as

$$f_{\text{mono}} = \frac{S_{\text{buffer}}}{S_{\text{micelles}}}, \text{ if } S_{\text{buffer}} < S_{\text{micelles}}, \text{ otherwise } f_{\text{mono}} = 1 \quad (5)$$

where  $S_{\text{micelles}}$  is the solubility in biorelevant media containing bile micelles and  $S_{\text{buffer}}$  is the solubility in the corresponding buffer without bile micelles.

When cyclodextrins are also present in the solution, eq 4 could be modified to get eq 6:

$$P_{UWL, \text{eff}} = \frac{D_{UWL, \text{eff}}}{h_{\text{eff}}} = \frac{(f_{\text{mono}} D_{UWL, \text{mono}} + f_{\text{mic}} D_{UWL, \text{mic}} + f_{\text{CD}} D_{UWL, \text{CD}})}{h_{\text{eff}}} \quad (6)$$

where  $f_{\text{CD}}$  is the fraction of the cyclodextrin complex bound molecule ( $f_{\text{mono}} + f_{\text{mic}} + f_{\text{CD}} = 1$ ) and  $D_{UWL, \text{CD}}$  is the diffusion coefficients of CD complex bound drug in the UWL. Equation 5 is modified to get eq 7:

$$f_{\text{mono}} = \frac{S_{\text{buffer}}}{S_{\text{micelles}} + \text{CD}}, \text{ if } S_{\text{buffer}} < S_{\text{micelles}} + \text{CD}, \text{ otherwise } f_{\text{mono}} = 1 \quad (7)$$

where  $S_{\text{micelles}} + \text{CD}$  is the solubility in biorelevant media containing not only bile micelles and lecithin but also cyclodextrin.

For the chosen parameters and assumptions, the diffusion coefficient of the free monomer ( $D_{\text{mono}}$ ) of ITRA and the cyclodextrin complex (assuming ITRA-cyclodextrin ratio 1:3)<sup>57,58</sup> was calculated using (eq 8).<sup>59</sup> The diffusion coefficient of the FaSSIF micelles was set as  $3.6 \times 10^{-7} \text{ cm}^2/\text{s}$  and as  $1.05 \times 10^{-6} \text{ cm}^2/\text{s}$  for the FeSSIF micelles. Considering that the mucus layer only slightly affects the diffusion coefficient at high taurocholate concentrations in the fed state, while in the fasted state the diffusion is slowed down by a factor of around three.<sup>10,60,61</sup>  $V_{GI, \text{fed}}/V_{GI, \text{fasted}}$  was considered to be equal to 1 during the calculations.

$$\log D_{UWL} = -4.14 - 0.417 \log M_w \quad (8)$$

**2.2.4. Estimation of Fraction Absorbed Ratio Based on Flux Results.** The fraction absorbed ( $F_a$ ) ratio for the prediction of food effect was calculated using eq 9:

$$F_a \text{ ratio} \approx \frac{J_{\text{fed}}}{J_{\text{fasted}}} \times \frac{V_{GI, \text{fed}}}{V_{GI, \text{fasted}}} \quad (9)$$

where  $J_{\text{fed}}$  and  $J_{\text{fasted}}$  are the measured flux with FeSSIF and FaSSIF being in the donor compartment, respectively.

The  $F_a$  ratio for the prediction of bioequivalence was calculated using eq 10:

$$F_a \text{ ratio} \approx \frac{J_{\text{test}}}{J_{\text{reference}}} \quad (10)$$

where test and reference are related to the flux measured for the test and reference drug product correspondingly.

**2.2.5. Calculation of Fraction Absorbed Ratios Based on in Vivo Data.** The  $F_a$  ratio for the prediction of food effect was calculated using eq 11:

$$F_a \text{ ratio} \approx \frac{AUC_{\text{fed}}}{AUC_{\text{fasted}}} \quad (11)$$

where  $AUC_{\text{fed}}$  and  $AUC_{\text{fasted}}$  are the area under the plasma concentration–time curve (24 h) in fed and fasted states.

The fraction of the reference dose absorbed ratio ( $F_{a, \text{ref}}$ ) for the prediction of bioequivalence was calculated using eq 12:

$$F_{a, \text{ref}} \text{ ratio} \approx \frac{AUC_{\text{test}}}{AUC_{\text{reference}}} \quad (12)$$

where  $AUC_{\text{test}}$  and  $AUC_{\text{reference}}$  are the area under the plasma concentration–time curve (24 h) for the test and reference products. When the 90% confidence interval of the ratio is between 0.80 and 1.25, the two products are expected to be bioequivalent.

Please note that the  $F_a$  ratio in itself contains dose considerations as well (eq 13). This means that, in the case of the formulations with different doses like SUBA-ITRA (test, 50 mg) and the Sporanox capsule (reference, 100 mg), a  $F_a$  ratio of 2 indicates bioequivalence.

$$F_a \text{ ratio} \approx \frac{AUC_{\text{test}}}{AUC_{\text{reference}}} \times \frac{\text{dose}_{\text{reference}}}{\text{dose}_{\text{test}}} \quad (13)$$

Since the criteria for bioequivalence is determined in AUC ratios (and  $C_{\text{max}}$  ratios), regardless of the dose,  $F_{a, \text{ref}}$  (eq 12) was calculated and used in this work for the bioequivalence prediction.

**2.2.6. Statistical Analyses.** Concentrations were expressed as means  $\pm$  SD and were compared using a two-sample Student's *t* test. Differences were considered statistically significant when  $p < 0.05$ .

### 3. RESULTS

First, the results of the different solubility measurements of pure ITRA in several aqueous media, with and without bile salts and formulation additives, are presented. Then the flux experiments of the marketed formulations of ITRA (Sporanox solution, Sporanox capsule, and SUBA-ITRA capsule) are described.

**3.1. Thermodynamic Solubility Assays.** Thermodynamic solubility measurements were carried out in several media (Table 2). The solubility result obtained in SGF was found to

**Table 2. Thermodynamic Solubility of ITRA in Different Aqueous Media Determined by the Saturation Shake Flask (SSF) Method**

media	SSF method ( $\mu\text{g/mL}$ )
pH 1.2 SGF	$5.4 \pm 0.44^a$
pH 5.0 FeSSIF blank	$<0.04^b$
pH 6.5 FaSSIF blank	$<0.04^{b,c}$
pH 7.4 ASB buffer	$114.5 \pm 0.58^a$

<sup>a</sup> $n = 3$ . <sup>b</sup>Under the detection limit of the spectrophotometer. <sup>c</sup>Intrinsic solubility.

be in good agreement with the literature data, suggesting around  $4 \mu\text{g/mL}$  solubility in  $0.1 \text{ M HCl}$  solution.<sup>62,63</sup> The solubility value measured in pH 7.4 ASB containing surfactants showed that sink conditions were ensured in the acceptor compartment during the flux measurement. In the case of pH 5 and 6.5 media the solubility of the API was so low that it was under the detection limit of the spectrophotometer. Therefore, in these cases, kinetic solubility measurements, which were expected to result in several times higher solubility values than the equilibrium thermodynamic solubility,<sup>28</sup> were chosen to determine the solubilizing effect of bile micelles and formulation additives on ITRA.

**3.2. Kinetic Solubility Measurements.** Kinetic solubility measurements were carried out in the same media as the donor media of the flux experiments (FaSSIF and FeSSIF) and also their respective blank media. Additional assays were done in FaSSIF and FeSSIF media in the presence of formulation additives used in marketed formulations of ITRA to evaluate the effect of these excipients on solubility. From the kinetic solubility results shown in Figure 3, it could be concluded that the FaSSIF and FeSSIF media were able to solubilize the API to the same level. It seemed that the addition of HPMC or HPMC-P only slightly changed the solubility of ITRA in FeSSIF and also in FaSSIF media. On the other hand, HP- $\beta$ -CD addition significantly increased the solubility of ITRA in both biorelevant media (in FaSSIF  $p < 0.001$ , in FeSSIF  $p < 0.001$ ). The increase was more prominent in FaSSIF than in FeSSIF, creating a significant difference between the solubility values obtained from the different buffers in the presence of cyclodextrin ( $p < 0.001$ ).

In the blank media, even the kinetic solubility of the drug was found to be under the detection limit of the spectrophotometer ( $40 \text{ ng/mL}$ ).

**3.3. Flux Experiments.** For simulating the pH change when the formulation goes from the stomach to the small

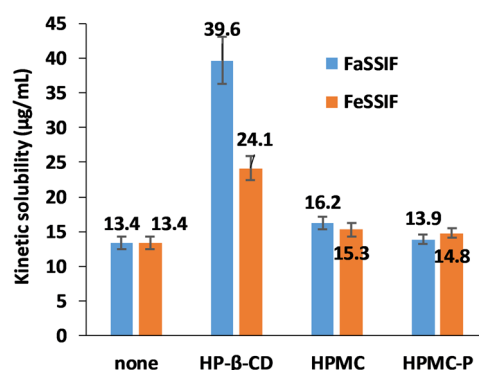


**Figure 3.** Kinetic solubility values determined in FaSSIF and FeSSIF media with or without additives.

intestine in a fasted state, a media change was carried out from SGF to FaSSIF. For the initial 30 min, the donor compartment was filled with SGF and the acceptor compartment was not yet connected to the donor. The dissolution of ITRA from the different formulations in the donor compartment for that period of time can be seen in Figure 4.a. ITRA added from Sporanox solution stayed fully dissolved in SGF ( $476 \mu\text{g/mL}$ ), no precipitation was observed. Sporanox capsule started releasing the API in SGF, but after reaching the maximum level of supersaturation, it started precipitating as well. The SUBA-ITRA capsule was only releasing a small amount of ITRA since HPMC-P, the matrix polymer of the ASD is not soluble in acidic media.

After 30 min, the media in the dissolution vessel was converted to fasted state simulated intestinal fluid and the acceptor compartment was added to the device. Changing the pH triggered immediate precipitation in the donor compartment for the Sporanox solution and further precipitation for the Sporanox capsule. The SUBA-ITRA capsule only disintegrated after the media change was conducted. In all three cases, the donor media became very turbid, disabling the *in situ* UV detection. For this reason, only the acceptor concentrations are presented in Figure 4b after media change. Early fluxes were calculated from the linear portion of the appearance profiles (50–120 min) (Figure 5). Although the dissolution and precipitation kinetics of the two capsules were quite different, the flux results obtained showed no significant difference (Figure 4b and Figure 5). The early flux of ITRA from Sporanox solution was found to be ca. 4 times higher in FaSSIF than any of the capsule forms (Figure 5).

For simulating the conditions after food intake in the gastrointestinal tract, FeSSIF media was used in the donor compartment. (No media change was carried out, and the acceptor compartment was assembled into the dissolution vessel from the beginning of the experiments, meaning the flux experiment started from time zero.) For all of the formulations, the donor media became very turbid right after the beginning of the experiment, disabling the *in situ* UV detection. For this reason, only the acceptor concentrations are presented in Figure 6. In the case of the capsules, similar early flux results were obtained, though the appearance profile of ITRA from the Sporanox capsule showed a decrease in flux after 2 h, while no change in flux was observed for the SUBA-ITRA capsule. These profiles suggest that ITRA dissolving from the SUBA-ITRA capsule is in a quite stable solution with a constant concentration of the drug present in the donor compartment,

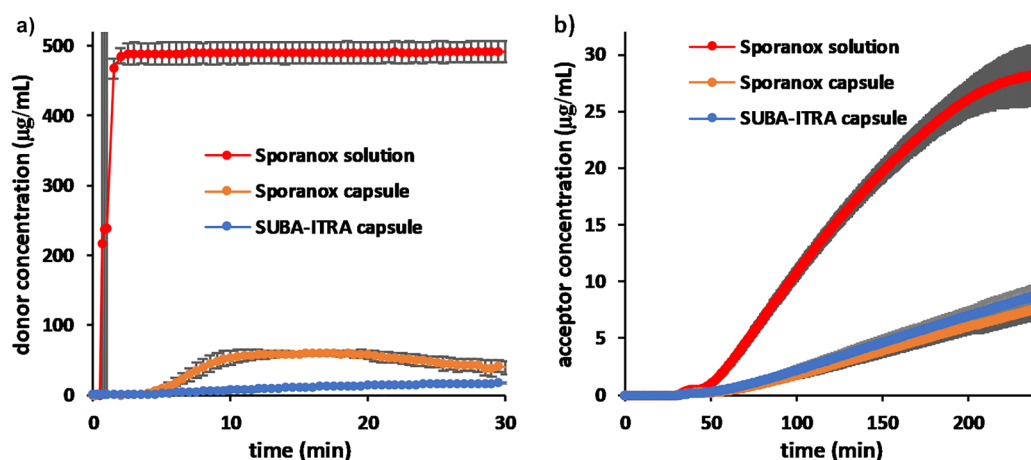


**Figure 4.** Dissolution in SGF (left) and appearance profile (right) of ITRA from Sporanox solution (100 mg), the Sporanox capsule (100 mg), and the SUBA-ITRA capsule (50 mg).

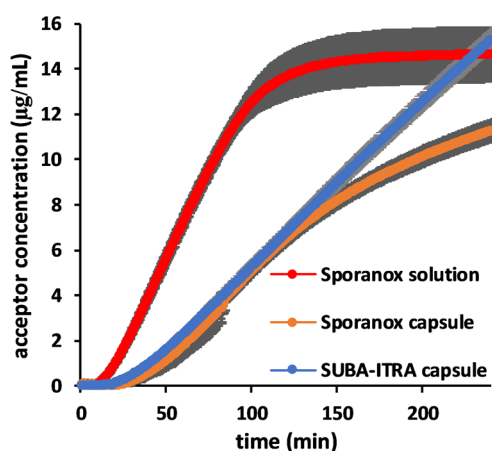


**Figure 5.** Early flux results of ITRA from Sporanox solution (100 mg), the Sporanox capsule (100 mg), and the SUBA-ITRA capsule (50 mg) (donor media: FaSSIF or FeSSIF).

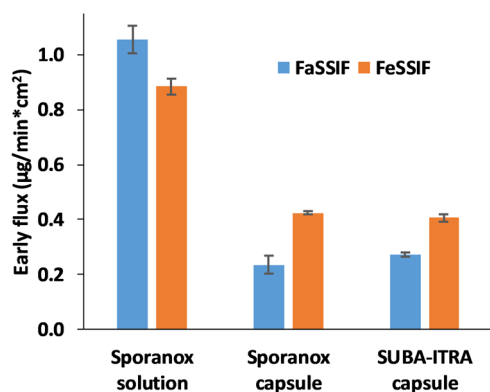


**Figure 6.** Appearance profile of ITRA from Sporanox solution (100 mg), the Sporanox capsule (100 mg), and the SUBA-ITRA capsule (50 mg) in FeSSIF media.

while ITRA dissolves and slowly precipitates from the Sporanox capsule in FeSSIF solution.

The early flux result of the API from its cyclodextrin-based solution was found to be superior to the capsule formulations in the fed state (Figure 5). The appearance profile of the Sporanox solution (decreasing flux) suggests precipitation in the donor media. The absolute value of the measured flux from

the Sporanox capsule in the fed state ( $0.424 \mu\text{g}/\text{min cm}^2$ ) was found to be in good agreement with previously reported *in vitro* flux experiments carried out in smaller scale dissolution–permeation setups.<sup>15,41</sup>

#### 4. DISCUSSION

$F_a$  ratios were calculated based on the results of the *in vitro* kinetic solubility assays, as well as the flux assays. These ratio values were examined on their ability to predict (1) the food effect on different ITRA formulations and (2) the bioequivalence test outcome comparing these formulations. All predictions were compared to *in vivo* results published by the European Medicines Agency (EMA) or the Food and Drug Administration (FDA).

**4.1. Prediction of Food Effect Based on *in Vitro* Kinetic Solubility and Flux Assays.** In the case of the Sporanox solution, the predicted  $F_a$  ratios showed a slightly negative (the ratio is less than 1) food effect, which is in good agreement with the *in vivo* data (Figure 7) and also the

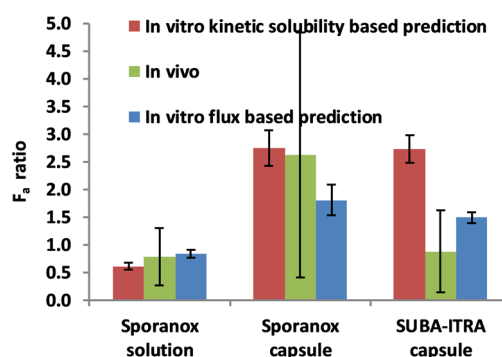


**Figure 7.** Comparison of the predicted fraction absorbed ratios (fed/fasted) for the estimation of food effect in the case of Sporanox solution, Sporanox capsules, and SUBA-ITRA capsules and the *in vivo* data.

recommendation to take the solution before meals.<sup>48</sup> Sporanox capsules are advised to be taken after a meal, which seems reasonable considering the *in vivo* results.<sup>47</sup> It can be seen from Figure 7 that both *in vitro*-based  $F_a$  calculations predict the *in vivo* behavior well (positive food effect,  $F_a$  ratio more than 1). It is interesting to see that, while positive food effect can be

easily seen from the flux results themselves (Figure 5), it is not so straightforward in the case of the kinetic solubility results (Figure 3). Since the kinetic solubility values do not differ significantly between fasted or fed states, the positive food effect can be explained by the fact that FeSSIF micelles are smaller than FaSSIF ones, and therefore diffuse around three times faster.<sup>10,60</sup> The difference in size and the diffusion coefficient explains why the results of the solubility-based prediction also indicate a significant positive food effect for the Sporanox capsule. In the case of the SUBA-ITRA capsule the manufacturer claimed to have found a reduced food effect as compared to the Sporanox capsule, and according to information in the patient leaflet, the drug can be taken regardless of meals.<sup>51</sup> Although the flux-based  $F_a$  ratio seems to show a slightly smaller food effect than the Sporanox capsule, according to *in vitro*-based predictions, a positive food effect can be anticipated.

**4.2. Prediction of Bioequivalence Based on *in Vitro* Flux and Kinetic Solubility Assays.** The SUBA-ITRA capsule containing half the ITRA dose of the brand capsule was found *in vivo* to be therapeutically equivalent but not bioequivalent to the Sporanox capsule, because of the significant difference obtained between the area under the concentration–time curve (AUC) values in the fasted state.<sup>51</sup> The  $F_{a,ref}$  ratio in the fasted state was calculated as a ratio of the AUC<sup>9</sup> of the test and reference product (eq 12) and was found to be 0.68 (Figure 8). Interestingly, the values of the maximum

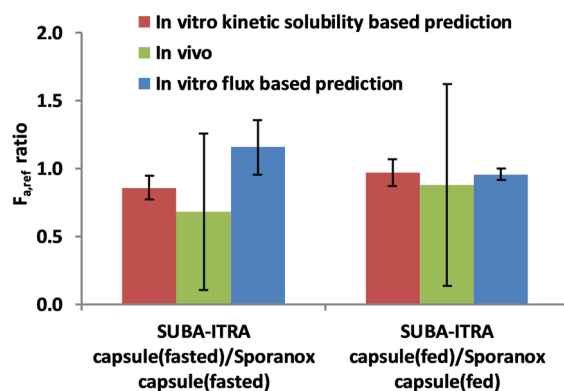


**Figure 8.** Predicted fraction absorbed ratios for the comparison of SUBA-ITRA (test) and Sporanox (reference) capsules in fasted and fed conditions and *in vivo* data from the bioequivalence study results.

concentration of the concentration–time curve ( $C_{max}$ ), and the time when the  $C_{max}$  is reached ( $t_{max}$ ), of each of the two formulations were found to be almost identical ( $C_{max}$  ratio = 0.99,  $t_{max}$  ratio = 1).<sup>51</sup> Based on both *in vitro* predictions,  $F_{a,ref}$  ratios around 1 were anticipated. From this comparison, it can be seen that both *in vitro*  $F_{a,ref}$  ratios are more in agreement with  $C_{max}$  ratios than AUC ratios. This seems to be rather logical since the flux values used in the calculations refer to the rate of absorption which can be expressed *in vivo* as  $C_{max}/t_{max}$ . Since  $t_{max}$  values were determined to be equal for both cases,  $C_{max}$  ratio can represent the *in vivo* initial rate of absorption. In many cases, not much difference can be seen in the AUC ratio and the  $C_{max}$  ratio during bioequivalence studies because very similar products with the same dose and identical or slightly different excipients are compared. While the composition of SUBA-ITRA ASD (HPMC-P instead of HPMC) might enable the rate of absorption to be very similar to the reference

product, the halved dose and short gastric retention time in the fasted state might be responsible for the significantly reduced AUC value. These effects cannot be modeled by the *in vitro* methods used in this study.

In the case of fed state studies *in vivo*, the  $F_{a,ref}$  ratio (SUBA-ITRA/Sporanox) is ca. 1 (0.88) (Figure 8), and the  $C_{max}$  values are also almost equivalent (ratio = 0.93),<sup>51</sup> suggesting a similar initial absorption rate. Both the kinetic solubility and flux-based predictions showed excellent agreement with the fed state *in vivo* results (Figure 8).

Sporanox solution and the Sporanox capsule were not compared in the fasted state in clinical studies published by the FDA, so the *in vivo* data shown in Figure 9 was taken from a

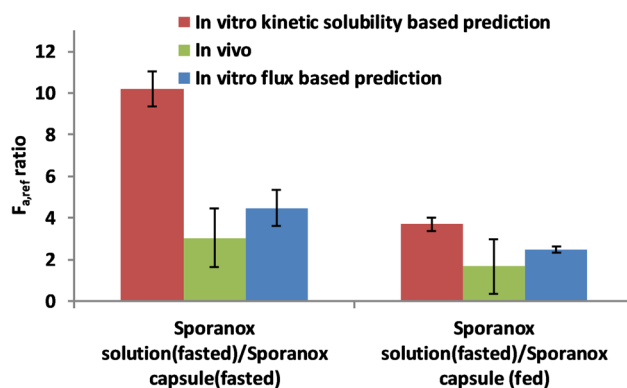


**Figure 9.** Predicted fraction absorbed ratios for the comparison Sporanox solution and Sporanox capsule in fasted and fed conditions and *in vivo* data.

publication by Brouwers et al.<sup>64</sup> In Figure 9, it can be seen that the flux-based  $F_{a,ref}$  ratio gives a fair estimate to the *in vivo* results, while kinetic solubility overestimates the positive effect of the cyclodextrin.

Sporanox solution was marketed 5 years after the capsule by Janssen Pharmaceutica. When launching the new formulation, it was compared to the capsule form.<sup>47</sup> Since it was already known that the solution was recommended to be taken before meals and that the solid formulation should be taken after a meal, Sporanox solution in the fasted state was compared to the Sporanox capsule in the fed state. (Figure 9) Both *in vitro*  $F_{a,ref}$  predictions showed superior bioavailability of ITRA from solution, which agreed well with the *in vivo* results. The *in vivo*  $F_{a,ref}$  ratio of ITRA from Sporanox solution was found to be ca. 2.5 times higher than from the capsule forms. Since the bioavailability of ITRA was greater from Sporanox solution, the solution and the capsule were therefore not bioequivalent products according to FDA.<sup>47</sup>

Comparing the two *in vitro*-based  $F_{a,ref}$  prediction approaches, it has to be noted that flux-based predictions were closer to the *in vivo* results when the HP- $\beta$ -CD containing solution and the HPMC containing a solid formulation were compared. This might be because *in vitro* kinetic solubility-based prediction requires that the diffusion coefficients of not just the bile micelles but also the cyclodextrin complexes are estimated. This estimate is highly dependent on the assumption of the HP- $\beta$ -CD–ITRA ratio (in this case, it was assumed to be 3:1).<sup>57</sup> Moreover, this model does not consider aggregation of CD complexes or any interplay between CD and bile micelles, although this may be possible according to the literature.<sup>65</sup> It must also be noted that the solubility-based



approach requires the investigation of solubility data in each media, both with and without the formulation additives, which is a more labor-intensive task than performing flux measurements.

It has to be noted that although no exact dissolution data was obtained due to the limitations of the fiber optic technique in extremely turbid media, it is possible to use manual sampling and offline analysis if needed in concert with the BioFLUX setup.

## 5. CONCLUSIONS

This study demonstrated that kinetic solubility and flux values measured under biorelevant conditions could be used as input parameters for biopharmaceutics modeling and simulations to estimate food effect and bioequivalence.

Both the kinetic solubility and the flux-based prediction methods were highly capable of determining the slightly negative food effect in the case of Sporanox solution, and a pronounced positive food effect for the Sporanox capsule. The flux-based method was able to predict even a positive, but slightly reduced food effect for the SUBA-ITRA capsule. Superior bioavailability was predicted when comparing Sporanox solution to the Sporanox capsule, which was found to be in good agreement with *in vivo* data published by the FDA. The limitations of *in vitro* methods were met when comparing the 50 mg SUBA-ITRA capsule to the 100 mg Sporanox capsule. Namely, the *in vitro* methods provided accurate information about the rate of absorption but were not able to predict the reduced AUC values caused by the halved dose and shorter gastric retention in the fasted state.

Comparing the *in vitro* flux and solubility-based  $F_a$  prediction methods, it was observed that, in the case of complex media containing bile micelles and cyclodextrins, it is advantageous to use the flux-based prediction. This model only uses the measured flux values, while solubility-based prediction requires accurate assumptions about the fraction of drug solubilized by micelles, complexation, and also the diffusivity of these species through the UWL.

It could also be concluded that the flux approach is less labor intensive, providing good IVIVC when compared to the solubility-based approach, especially in the case of complex formulations and biorelevant media.

## AUTHOR INFORMATION

### Corresponding Authors

\*E-mail: [borbas.eniko@mail.bme.hu](mailto:borbas.eniko@mail.bme.hu). Phone: +36-1463-1424.

\*E-mail: [bsinko@pion-inc.com](mailto:bsinko@pion-inc.com).

### ORCID

Enikő Borbás: 0000-0002-9393-9978

Hajnalka Pataki: 0000-0002-8103-0601

### Author Contributions

The manuscript was written through the contributions of all authors. All authors have given approval to the final version of the manuscript.

### Funding

This project was supported by the ÚNKP-18-3-I, ÚNKP-18-4-BME-213 New National Excellence Program of the Ministry of Human Capacities, Gedeon Richter Talentum Foundation, Pro Progressio Foundation and Hungarian Scientific Research Fund (OTKA PD121143). This work was performed in the frame of FIEK\_16-1-2016-0007 project, implemented with the support provided from the National Research, Development

and Innovation Fund of Hungary, financed under the FIEK\_16 funding scheme. Hajnalka Pataki is thankful for the János Bolyai Research Scholarship of the Hungarian Academy of Sciences.

## Notes

The authors declare no competing financial interest.

## ABBREVIATIONS

ITRA, itraconazole; ASD, amorphous solid dispersion; API, active pharmaceutical ingredient; BCS, biopharmaceutics classification system; UWL, unstirred water layer;  $F_a$ , fraction of dose absorbed; AUC, area under the plasma concentration–time curve;  $C_{max}$ , maximum concentration of the plasma concentration–time curve;  $t_{max}$ , the time when  $C_{max}$  is reached; EMA, European Medicines Agency; FDA, Food and Drug Administration; HPMC, hydroxypropylmethylcellulose; HPMC-P, hydroxypropylmethylcellulose-phthalate, HP- $\beta$ -CD, (2-hydroxypropyl)- $\beta$ -cyclodextrin; FO probe, fiber-optic probe; SSF, saturation shake flask; SGF, simulated gastric fluid; FaSSIF, fasted state simulated intestinal fluid; FeSSIF, fed state simulated intestinal fluid; ASB, acceptor sink buffer

## REFERENCES

- (1) Hens, B.; Sinko, P. D.; Job, N.; Dean, M.; Al-Gousous, J.; Salehi, N.; Ziff, R. M.; Tsume, Y.; Bermejo, M.; Paixão, P.; et al. Formulation Predictive Dissolution (FPD) Testing to Advance Oral Drug Product Development: An Introduction to the US FDA Funded '21st Century BA/BE' Project. *Int. J. Pharm.* **2018**, *548* (1), 120–127.
- (2) Bergström, C. A. S.; Holm, R.; Jørgensen, S. A.; Andersson, S. B. E.; Artursson, P.; Beato, S.; Borde, A.; Box, K.; Brewster, M.; Dressman, J.; et al. Early Pharmaceutical Profiling to Predict Oral Drug Absorption: Current Status and Unmet Needs. *Eur. J. Pharm. Sci.* **2014**, *57* (1), 173–199.
- (3) Sugano, K.; Terada, K. Rate- and Extent-Limiting Factors of Oral Drug Absorption: Theory and Applications. *J. Pharm. Sci.* **2015**, *104* (9), 2777–2788.
- (4) Borbás, E.; Tőzsér, P.; Tsinman, K.; Tsinman, O.; Takács-Novák, K.; Völgyi, G.; Sinkó, B.; Nagy, Z. K. Effect of Formulation Additives on Drug Transport through Size-Exclusion Membranes. *Mol. Pharmaceutics* **2018**, *15* (8), 3308–3317.
- (5) Dahan, A.; Miller, J. M. The Solubility-Permeability Interplay and Its Implications in Formulation Design and Development for Poorly Soluble Drugs. *AAPS J.* **2012**, *14* (2), 244–251.
- (6) Loftsson, T.; Brewster, M. E. Pharmaceutical Applications of Cyclodextrins: Effects on Drug Permeation through Biological Membranes. *J. Pharm. Pharmacol.* **2011**, *63* (9), 1119–1135.
- (7) Dahan, A.; Miller, J. M.; Hoffman, A.; Amidon, G. E.; Amidon, G. L. The Solubility-Permeability Interplay in Using Cyclodextrins as Pharmaceutical Solubilizers: Mechanistic Modeling and Application to Progesterone. *J. Pharm. Sci.* **2010**, *99* (6), 2739–2749.
- (8) Fenyvesi, F.; Kiss, T.; Fenyvesi, E.; Szenté, L.; Veszelka, S.; Deli, M. A.; Váradi, J.; Fehér, P.; Ujhelyi, Z.; Tószaki, A.; et al. Randomly Methylated  $\beta$ -cyclodextrin Derivatives Enhance Taxol Permeability through Human Intestinal Epithelial Caco-2 Cell Monolayer. *J. Pharm. Sci.* **2011**, *100* (11), 4734–4744.
- (9) Sugano, K.; Kataoka, M.; Da Costa Mathews, C.; Yamashita, S. Prediction of Food Effect by Bile Micelles on Oral Drug Absorption Considering Free Fraction in Intestinal Fluid. *Eur. J. Pharm. Sci.* **2010**, *40*, 118–124.
- (10) Sugano, K. Estimation of Effective Intestinal Membrane Permeability Considering Bile Micelle Solubilisation. *Int. J. Pharm.* **2009**, *368* (1–2), 116–122.
- (11) Fagerholm, U.; Lennernäs, H. Experimental Estimation of the Effective Unstirred Water Layer Thickness in the Human Jejunum, and Its Importance in Oral Drug Absorption. *Eur. J. Pharm. Sci.* **1995**, *3* (5), 247–253.



- (12) Avdeef, A.; Bendels, S.; Di, L. i.; Faller, B.; Kansy, M.; Sugano, K.; Yamauchi, Y. PAMPA—Critical Factors for Better Predictions of Absorption. *J. Pharm. Sci.* **2007**, *96* (11), 2893–2909.
- (13) Sugano, K.; Nabuchi, Y.; Machida, M.; Aso, Y. Prediction of Human Intestinal Permeability Using Artificial Membrane Permeability. *Int. J. Pharm.* **2003**, *257* (1–2), 245–251.
- (14) Stewart, A. M.; Grass, M. E.; Brodeur, T. J.; Goodwin, A. K.; Morgen, M. M.; Friesen, D. T.; Vodak, D. T. Impact of Drug-Rich Colloids of Itraconazole and HPMCAS on Membrane Flux In Vitro and Oral Bioavailability in Rats. *Mol. Pharmaceutics* **2017**, *14* (7), 2437–2449.
- (15) Stewart, A. M.; Grass, M. E.; Mudie, D. M.; Morgen, M. M.; Friesen, D. T.; Vodak, D. T. Development of a Biorelevant, Material-Sparing Membrane Flux Test for Rapid Screening of Bioavailability-Enhancing Drug Product Formulations. *Mol. Pharmaceutics* **2017**, *14* (6), 2032–2046.
- (16) Yamaguchi, T.; Ikeda, C.; Sekine, Y. Intestinal Absorption of a Beta-Adrenergic Blocking Agent Nadolol. I. Comparison of Absorption Behavior of Nadolol with Those of Other Beta-Blocking Agents in Rats. *Chem. Pharm. Bull.* **1986**, *34* (8), 3362–3369.
- (17) Yamaguchi, T.; Oida, T.; Ikeda, C.; Sekine, Y. Intestinal Absorption of a Beta-Adrenergic Blocking Agent Nadolol. III. Nuclear Magnetic Resonance Spectroscopic Study on Nadolol-Sodium Cholate Micellar Complex and Intestinal Absorption of Nadolol Derivatives in Rats. *Chem. Pharm. Bull.* **1986**, *34* (10), 4259–4264.
- (18) Beig, A.; Miller, J. M.; Lindley, D.; Carr, R. A.; Zocharski, P.; Agbaria, R.; Dahan, A. Head-To-Head Comparison of Different Solubility-Enabling Formulations of Etoposide and Their Consequent Solubility-Permeability Interplay. *J. Pharm. Sci.* **2015**, *104*, 2941–2947.
- (19) Yamaguchi, T.; Ikeda, C.; Sekine, Y. Intestinal Absorption of a Beta-Adrenergic Blocking Agents Nadolol. II. Mechanism of the Inhibitory Effect on the Intestinal Absorption of Nadolol by Sodium Cholate in Rats. *Chem. Pharm. Bull.* **1986**, *34* (9), 3836–3843.
- (20) Poelma, F. G.; Breäs, R.; Tukker, J. J.; Crommelin, D. J. Intestinal Absorption of Drugs. The Influence of Mixed Micelles on the Disappearance Kinetics of Drugs from the Small Intestine of the Rat. *J. Pharm. Pharmacol.* **1991**, *43* (5), 317–324.
- (21) Lennernäs, H.; Regårdh, C. G. Evidence for an Interaction between the Beta-Blocker Pafenolol and Bile Salts in the Intestinal Lumen of the Rat Leading to Dose-Dependent Oral Absorption and Double Peaks in the Plasma Concentration-Time Profile. *Pharm. Res.* **1993**, *10* (6), 879–883.
- (22) Ingels, F.; Beck, B.; Oth, M.; Augustijns, P. Effect of Simulated Intestinal Fluid on Drug Permeability Estimation across Caco-2 Monolayers. *Int. J. Pharm.* **2004**, *274* (1–2), 221–232.
- (23) Loftsson, T. Drug Permeation through Biomembranes: Cyclodextrins and the Unstirred Water Layer. *Pharmazie* **2012**, *67* (5), 363–370.
- (24) Avdeef, A.; Kansy, M.; Bendels, S.; Tsinman, K. Absorption-Excipient-PH Classification Gradient Maps: Sparingly Soluble Drugs and the PH Partition Hypothesis. *Eur. J. Pharm. Sci.* **2008**, *33*, 29.
- (25) Dahan, A.; Beig, A.; Ioffe-Dahan, V.; Agbaria, R.; Miller, J. M. The Twofold Advantage of the Amorphous Form as an Oral Drug Delivery Practice for Lipophilic Compounds: Increased Apparent Solubility and Drug Flux Through the Intestinal Membrane. *AAPS J.* **2013**, *15* (2), 347–353.
- (26) Dahan, A.; Beig, A.; Lindley, D.; Miller, J. M. The Solubility-Permeability Interplay and Oral Drug Formulation Design: Two Heads Are Better than One. *Adv. Drug Delivery Rev.* **2016**, *101*, 99–107.
- (27) Sugano, K. Computational Oral Absorption Simulation for Low-Solubility Compounds. *Chem. Biodiversity* **2009**, *6* (2009), 2014–2029.
- (28) Box, K. J.; Volgyi, G.; Baka, E.; Stuart, M.; Takacs-Novak, K.; Comer, J. E.A. Equilibrium versus Kinetic Measurements of Aqueous Solubility, and the Ability of Compounds to Supersaturate in Solution-A Validation Study. *J. Pharm. Sci.* **2006**, *95* (6), 1298–1307.
- (29) Almeida, L.; Reutzel-Edens, S. M.; Stephenson, G. A.; Taylor, L. S. Assessment of the Amorphous “Solubility” of a Group of Diverse Drugs Using New Experimental and Theoretical Approaches. *Mol. Pharmaceutics* **2015**, *12* (2), 484–495.
- (30) Borbás, E.; Sinkó, B.; Tsinman, O.; Tsinman, K.; Kiserdei, É.; Démuth, B.; Balogh, A.; Bodák, B.; Domokos, A.; Dargó, G.; et al. Investigation and Mathematical Description of the Real Driving Force of Passive Transport of Drug Molecules from Supersaturated Solutions. *Mol. Pharmaceutics* **2016**, *13* (11), 3816–3826.
- (31) Warren, D. B.; Bergström, C. A. S.; Benameur, H.; Porter, C. J. H.; Pouton, C. W. Evaluation of the Structural Determinants of Polymeric Precipitation Inhibitors Using Solvent Shift Methods and Principle Component Analysis. *Mol. Pharmaceutics* **2013**, *10* (8), 2823–2848.
- (32) Raina, S. A.; Zhang, G. G. Z.; Alonzo, D. E.; Wu, J.; Zhu, D.; Catron, N. D.; Gao, Y.; Taylor, L. S. Impact of Solubilizing Additives on Supersaturation and Membrane Transport of Drugs. *Pharm. Res.* **2015**, *32*, 3350–3364.
- (33) Indulkar, A. S.; Box, K. J.; Taylor, R.; Ruiz, R.; Taylor, L. S. PH-Dependent Liquid - Liquid Phase Separation of Highly Supersaturated Solutions of Weakly Basic Drugs. *Mol. Pharmaceutics* **2015**, *12* (7), 2365–2377.
- (34) Hsieh, Y. L.; Ilievbare, G. A.; Van Eerdenbrugh, B.; Box, K. J.; Sanchez-Felix, M. V.; Taylor, L. S. PH-Induced Precipitation Behavior of Weakly Basic Compounds: Determination of Extent and Duration of Supersaturation Using Potentiometric Titration and Correlation to Solid State Properties. *Pharm. Res.* **2012**, *29* (10), 2738–2753.
- (35) Emami Riedmaier, A.; Lindley, D. J.; Hall, J. A.; Castleberry, S.; Slade, R. T.; Stuart, P.; Carr, R. A.; Borchardt, T. B.; Bow, D. A. J.; Nijssen, M. Mechanistic Physiologically Based Pharmacokinetic Modeling of the Dissolution and Food Effect of a Biopharmaceutics Classification System IV Compound—The Venetoclax Story. *J. Pharm. Sci.* **2018**, *107* (1), 495–502.
- (36) Buckley, S. T.; Fischer, S. M.; Fricker, G.; Brandl, M. In Vitro Models to Evaluate the Permeability of Poorly Soluble Drug Entities: Challenges and Perspectives. *Eur. J. Pharm. Sci.* **2012**, *45* (3), 235–250.
- (37) Berben, P.; Bauer-Brandl, A.; Brandl, M.; Faller, B.; Flaten, G. E.; Jacobsen, A. C.; Brouwers, J.; Augustijns, P. Drug Permeability Profiling Using Cell-Free Permeation Tools: Overview and Applications. *Eur. J. Pharm. Sci.* **2018**, *119* (March), 219–233.
- (38) Avdeef, A.; Tsinman, O. PAMPA- A Drug Absorption In Vitro Model 13. Chemical Selectivity Due to Membrane Hydrogen Bonding: In Combo Comparisons of HDM-, DOPC-, and DS-PAMPA Models. *Eur. J. Pharm. Sci.* **2006**, *28* (1–2), 43–50.
- (39) Borbás, E.; Balogh, A.; Bocz, K.; Müller, J.; Kiserdei, É.; Vigh, T.; Sinkó, B.; Marosi, A.; Halász, A.; Dohányos, Z.; et al. In Vitro Dissolution-Permeation Evaluation of an Electrospun Cyclodextrin-Based Formulation of Aripiprazole Using MFlux<sup>TM</sup>. *Int. J. Pharm.* **2015**, *491* (1), 180–189.
- (40) Borbás, E.; Nagy, Z. K.; Nagy, B.; Balogh, A.; Farkas, B.; Tsinman, O.; Tsinman, K.; Sinkó, B. The Effect of Formulation Additives on in Vitro Dissolution-Absorption Profile and in Vivo Bioavailability of Telmisartan from Brand and Generic Formulations. *Eur. J. Pharm. Sci.* **2018**, *114*, 310–317.
- (41) Tsinman, K.; Tsinman, O.; Lingamaneni, R.; Zhu, S.; Riebeschl, B.; Grandeur, A.; Juhnke, M.; Van Eerdenbrugh, B. Ranking Itraconazole Formulations Based on the Flux through Artificial Lipophilic Membrane. *Pharm. Res.* **2018**, *35* (8), 1–13.
- (42) Li, J.; Tsinman, K.; Tsinman, O.; Wigman, L. Using PH Gradient Dissolution with In-Situ Flux Measurement to Evaluate Bioavailability and DDI for Formulated Poorly Soluble Drug Products. *AAPS PharmSciTech* **2018**, *19* (7), 2898–2907.
- (43) McConnell, E. L.; Fadda, H. M.; Basit, A. W. Gut Instincts: Explorations in Intestinal Physiology and Drug Delivery. *Int. J. Pharm.* **2008**, *364* (2), 213–226.
- (44) Yu, L. X.; Amidon, G. L.; Polli, J. E.; Zhao, H.; Mehta, M. U.; Conner, D. P.; Shah, V. P.; Lesko, L. J.; Chen, M.-L.; Lee, V. H. L.;

et al. Biopharmaceutics Classification System: The Scientific Basis for Biowaiver Extensions. *Pharm. Res.* **2002**, 19 (7), 921–925.

(45) Ruell, J. A.; Tsinman, O.; Avdeef, A. Acid-Base Cosolvent Method for Determining Aqueous Permeability of Amiodarone, Itraconazole, Tamoxifen, Terfenadine and Other Very Insoluble Molecules. *Chem. Pharm. Bull.* **2004**, 52 (5), 561–565.

(46) Gilis, P. M. V.; De Condé, V. F. V.; Vandecruys, R. P. G. *Beads Having a Core Coated with an Antifungal and a Polymer*, US Patent 005633014A, March 18, 1997.

(47) FDA. Patient Information of Sporanox (Itraconazole) Capsules. [https://www.accessdata.fda.gov/drugsatfda\\_docs/label/2009/020083s040s041s044lbl.pdf](https://www.accessdata.fda.gov/drugsatfda_docs/label/2009/020083s040s041s044lbl.pdf) (accessed 02/01/2019).

(48) FDA. Patient Information of Sporanox (Itraconazole) Oral Solution. [https://www.accessdata.fda.gov/drugsatfda\\_docs/label/2011/020657s025lbl.pdf](https://www.accessdata.fda.gov/drugsatfda_docs/label/2011/020657s025lbl.pdf) (accessed 02/01/2019).

(49) Shin, J. H.; Choi, K. Y.; Kim, Y. C.; Lee, M. G. Dose-Dependent Pharmacokinetics of Itraconazole after Intravenous or Oral Administration to Rats: Intestinal First-Pass Effect. *Antimicrob. Agents Chemother.* **2004**, 48 (5), 1756–1762.

(50) Yoo, S. D.; Lee, S. H.; Kang, E.; Jun, H.; Jung, J. Y.; Park, J. W.; Lee, K. H. Bioavailability of Itraconazole in Rats and Rabbits after Administration of Tablets Containing Solid Dispersion Particles. *Drug Dev. Ind. Pharm.* **2000**, 26 (1), 27–34.

(51) MHRA. Public Assessment Report of Lozanoc. <http://www.mhra.gov.uk/home/groups/par/documents/websiteresources/con249676.pdf> (accessed 02/01/2019).

(52) Mayne Pharma. <http://www.maynepharm.com/our-capabilities/specialty-technologies/suba-bioavailability-technology/>.

(53) Baka, E.; Comer, J. E. A.; Takács-Novák, K. Study of Equilibrium Solubility Measurement by Saturation Shake-Flask Method Using Hydrochlorothiazide as Model Compound. *J. Pharm. Biomed. Anal.* **2008**, 46 (2), 335–341.

(54) Avdeef, A.; Fuguet, E.; Llinàs, A.; Ràfols, C.; Bosch, E.; Völgyi, G.; Verbić, T.; Boldyreva, E.; Takács-Novák, K. Equilibrium Solubility Measurement of Ionizable Drugs - Consensus Recommendations for Improving Data Quality. *ADMET DMPK* **2016**, 4 (2), 117–178.

(55) Bendels, S.; Tsinman, O.; Wagner, B. R.; Lipp, D.; Parrilla, I.; Kansy, M.; Avdeef, A. PAMPA-Excipient Classification Gradient Map. *Pharm. Res.* **2006**, 23 (11), 2525–2535.

(56) FDA. [https://www.accessdata.fda.gov/scripts/cder/dissolution/dsp\\_getallData.cfm](https://www.accessdata.fda.gov/scripts/cder/dissolution/dsp_getallData.cfm) (accessed 20/06/2019).

(57) Peeters, J.; Neeskens, P.; Tollenaere, J. P.; Van Remoortere, P.; Brewster, M. E. Characterization of the Interaction of 2-hydroxypropyl- $\beta$ -cyclodextrin with Itraconazole at PH 2, 4, and 7. *J. Pharm. Sci.* **2002**, 91 (6), 1414–1422.

(58) Fenyvesi, É. Itraconazole/HPBCD Solution 20 Years on the Market. *Cyclodext. News* **2017**, 31 (8–9), 1.

(59) Avdeef, A. Physicochemical Profiling (Solubility, Permeability and Charge State). *Curr. Top. Med. Chem.* **2001**, 1 (4), 277–351.

(60) Li, C.-Y.; Zimmerman, C.-L.; Wiedmann, T. S. Diffusivity of Bile Salt/Phospholipid Aggregates in Mucin. *Pharm. Res.* **1996**, 13 (4), 535–541.

(61) Wagner, J. G. Method of Estimating Relative Absorption of a Drug in a Series of Clinical Studies in Which Blood Levels Are Measured after Single and/or Multiple Doses. *J. Pharm. Sci.* **1967**, 56 (5), 652–653.

(62) Matsui, K.; Tsume, Y.; Amidon, G. E.; Amidon, G. L. The Evaluation of In Vitro Drug Dissolution of Commercially Available Oral Dosage Forms for Itraconazole in Gastrointestinal Simulator With Biorelevant Media. *J. Pharm. Sci.* **2016**, 105 (9), 2804–2814.

(63) Ghazal, H. S.; Dyas, A. M.; Ford, J. L.; Hutcheon, G. A. In Vitro Evaluation of the Dissolution Behaviour of Itraconazole in Bio-Relevant Media. *Int. J. Pharm.* **2009**, 366 (1–2), 117–123.

(64) Brouwers, J.; Geboers, S.; Mols, R.; Tack, J.; Augustijns, P. Gastrointestinal Behavior of Itraconazole in Humans - Part 1: Supersaturation from a Solid Dispersion and a Cyclodextrin-Based Solution. *Int. J. Pharm.* **2017**, 525 (1), 211–217.

(65) Stappaerts, J.; Augustijns, P. Displacement of Itraconazole from Cyclodextrin Complexes in Biorelevant Media: In Vitro Evaluation of

Supersaturation and Precipitation Behavior. *Int. J. Pharm.* **2016**, 511 (1), 680–687.